On the use of satellite data in a general circulation ocean model: altimeter and scatterometer data

Assimilation
Altimeter
Scatterometer
Numerical simulations
Eddies

Assimilation
Altimètre
Diffusiomètre
Simulations numériques
Tourbillons

Moncef BOUKTHIR, Jacques VERRON and Bernard BARNIER

Laboratoire des Écoulements Géophysiques et Industriels, Institut de Mécanique de Grenoble, BP 53 X, 38041 Grenoble Cedex, France.

ABSTRACT

This paper examines how satellite altimeter and scatterometer measurements could be jointly used in a numerical ocean model in an attempt to simulate a realistic ocean circulation. The aim of the study is to determine quantitatively how sensitive the efficiency of the assimilation process may be to the variability of the wind stress curl and to evaluate the ability of the Topex/Poseidon altimetric data to correct for the sampling of scatterometer wind data that is to be provided by the forthcoming ERS1 and NSCAT satellite missions.

The model is quasigeostrophic, eddy-resolving and multi-layered, and is applied to the prognostic description of the mid-latitude ocean circulation in a schematic box ocean. Satellite altimeter data are simulated from model runs (forced by ECMWF winds) under the conditions of the Topex/Poseidon mission and are assimilated into the model by using a Newtonian relaxation or nudging technique. Satellite scatterometer wind data are simulated from ECMWF daily analyses of the wind stress over the North Atlantic.

The use of realistic winds varying over a large range of temporal and spatial scales clearly has important dynamical consequences for the resulting ocean circulation but also militates against the efficiency of the altimeter data assimilation. The insertion of the altimeter data into the model is still able to constrain strongly the slow baroclinic circulation. However, the high frequency forcing generates barotropic Rossby waves that dominate the instantaneous flow throughout the basin and prevent complete convergence in the barotropic mode. Nevertheless, by smoothing out this fast time variability it is demonstrated that the assimilation of the altimeter data is still efficient in driving the larger time scales of the model ocean circulation.

When performing altimeter data assimilation into a model domain forced by scatterometer wind data, the efficiency of the assimilation process is only slightly diminished but remains globally equivalent to the true wind forcing situation. Different ways of assimilating altimeter data were tested; they revealed that the use of the sea-level instead of the vorticity is more favorable; this result was not observed when model forcing did not incorporate such variability, *i. e.* when it was schematized by large scale constant wind stress curl (Verron, 1991).

Oceanologica Acta, 1992. **15**, 5, 507-523.

RÉSUMÉ

Utilisation conjointe de données altimétriques et diffusiométriques dans un modèle de circulation générale océanique

Le cadre général de cette étude est l'utilisation conjointe de données satellitaires provenant d'instruments différents pour forcer les modèles de circulation générale océanique. Le travail présenté dans cet article a pour but de quantifier la sensi-

bilité du processus d'assimilation des mesures de la dénivellation de la surface libre océanique fournies par l'altimétrie satellitaire (mission Topex-Poséidon) dans un modèle d'océan, aux échantillonnages de vent que fourniront les diffusiomètres des missions ERS-1 et NSCAT.

Le modèle d'océan est quasi-géostrophique, stratifié en couches, et sa résolution horizontale est suffisamment fine pour résoudre explicitement les tourbillons de moyenne échelle. Il est appliqué, dans une géométrie schématique en boite carrée, à la description de l'évolution temporelle de la circulation océanique aux latitudes moyennes. Les données altimétriques satellitaires sont simulées à partir de résultats de l'intégration du modèle, dans les conditions de la mission Topex-Poseidon. L'assimilation des données altimétriques simulées est faite par la technique du «nudging». Le rotationnel de vent qui force le modèle est dérivé des analyses journalières des tensions de vent sur l'Atlantique Nord que produit le Centre Européen de Prévision Météorologique à Moyen Terme (CEPMMT). Ces tensions sont également utilisées pour simuler les forçages de vent diffusiométriques dans le cadre des missions ERS-1 et NSCAT.

L'utilisation d'un forçage de vent dont la variabilité couvre une large gamme d'échelles spatiales et temporelles, au lieu d'un forçage climatologique constant, a manifestement d'importantes conséquences sur la réponse du modèle, et a un effet défavorable sur l'efficacité de l'assimilation des données altimétriques. En effet, si l'assimilation de données de dénivellation de la surface océanique sous la trace du satellite a toujours la capacité de contraindre les modes baroclines vers plus de réalisme, ce n'est pas le cas pour le mode barotrope. Les hautes fréquences du forçage (périodes inférieures à la semaine) engendrent des ondes de Rossby barotropes rapides qui sont responsables de la divergence partielle de l'assimilation du mode externe. Cependant, on montre qu'un lissage temporel de cette variabilité haute fréquence permet une convergence satisfaisante de l'assimilation pour tous les modes du modèle.

Lorsque les expériences d'assimilation des données altimétriques sont effectuées avec les vents diffusiométriques, les résultats sont légèrement dégradés mais l'impact de l'assimilation sur la circulation résultante du modèle reste cependant très positif.

Différents modes d'insertion de la donnée altimétrique ont également été testés. Il apparait que l'usage direct de la dénivellation de la surface libre est plus efficace que celui de la vorticité tronquée. Ce résultat n'etait pas apparu lors d'études similaires avec des vents constants. Il semble donc que les effets liés à la variabilité du vent sont mieux pris en compte si la variable assimilée dans le modèle est la dénivellation de la surface libre océanique.

Oceanologica Acta, 1992. **15**, 5, 507-523.

INTRODUCTION

In contrast with meteorological data, available *in situ* oceanographic data are sparsely scattered both in time and space. With forthcoming satellite missions dedicated to oceanography, it is to be hoped that our knowledge of the world's oceans will undergo a substantial increase over the next decade. Synoptic mapping of sea surface height variability and wind-stress intensity and direction should become available, for example, from sources such as Topex/Poseidon, ERS1, ERS2 and NSCAT. These quasi-synoptic ocean data will, however, be available only for the surface, and ocean models will thus have an essential role to play in resolving the deep circulation and in covering the intermediate scales unrepresented in the altimetric data. Consequently, ocean models and assimilation techniques will have to be carefully designed for the successfull extrapolation of surface information downwards in order to recreate realistic ocean circulation.

Several studies have already examined the possibility of dynamically transferring information on topographic height into the deep ocean flow. Verron and Holland (1989) used a quasi-geostrophic eddy-resolving model to perform data assimilation tests and adapted a simple technique of assimilation which is quite effective in reconstructing the four-dimensional ocean circulation. They showed how the nudging technique, which acts as a Newtonian relaxation on the surface vorticity field, works to make the different modes converge towards the observations and to recreate satisfactory abyssal flows. Holland and Malanotte-Rizzoli (1989) studied the effect of changing space and/or time resolution on the assimilation of the surface height

data. Verron (1990] performed assimilation tests using realistic sampling along tracks in order to determine the optimal conditions for satellite missions.

Uncertainty with regard to the determination of the geoid is a major obstacle to the use of altimetric data for ocean circulation purposes. There is little chance that this will be remedied in the near future by the availability of highly accurate geoid data. One method that has been proposed for avoiding the effects of geoid uncertainties is the use of temporal differences in the data, either along repeat tracks or at points where ascending and descending orbital passes cross. Miller (1989) derived the Kalman filter for this special case and discussed whether temporal differences alone are sufficient to determine the model state uniquely. In the case of non linear systems, Miller's main conclusion was that if the time lag between observations is so long that the fields at successive times become uncorrelated, there will be no hope in assimilating temporal differences directly. White *et al.* (1990) assimilated simulated Geosat sea-level time-differences using the method of optimal interpolation. Their results show that the assimilation of altimetric sea level differences into the model is capable of constraining the mesoscale eddy activity successfully when the dynamics are mostly linear, but not in the case of strongly nonlinear dynamics. The recent study by Verron (1991) shows that the nudging technique applied to the time difference in sea-level exhibits similar results which are explained by the phasing of the assimilation process.

Preliminary studies making use of altimeter measurements show that the reliability of the residuals of the altimeter signal is adequate for constraining the ocean eddy variability Verron *et al.* (this issue). But this reliability is clearly insufficient for the mean signal because of geoid uncertainties and orbit errors. Therefore, the model prediction for the mean circulation cannot be constrained by altimeter data except perhaps in a handful of regions where the mean circulation is associated with eddy variability (eddy-driven mean circulation). The model itself should then be able to provide the most reliable mean sea-level possible. In this regard, an adequate knowledge of the wind stress appears to be crucial and this is a powerful argument for the joint use of altimeter and scatterometer wind data.

Several recent developments point to the necessity of examining the detailed nature of wind stress, in particular with respect to the manner in which the ocean model responds to forcing at high frequencies and/or wave numbers. Using a flat-bottomed, 8-layer, linear QG model of the North Pacific Ocean, Large *et al.* (1991) showed that high frequency forcing produces higher kinetic energy at all depths and, when forced with a thirty-day averaged wind stress curl, the interannual streamfunction variance is typically only 30 % of its value when forced with two-day or shorter averages. Barnier *et al.* (1991) discussed the ability of scatterometer winds successfully to force a numerical ocean model. Their conclusions were that scatterometer wind data seem appropriate for ocean modeling purposes without their prior assimilation into meteorological models. Objective mapping is, however, necessary to fill the gaps arising from the patchiness and irregular resolution of the swaths.

The present study addresses at the appropriateness of conducting several future missions simultaneously where altimeter (Topex/Poseidon) and scatterometer (ERS1, ERS2 and NSCAT) data will be available over the world oceans. Numerical experiments are performed using both altimeter data and scatterometer wind data to investigate how much each of them can contribute to recreate the ocean circulation and determine their complementary contributions. A preliminary question is how sensitive the efficiency of the assimilation may be when wind stress-curl variability is included in the model ocean, since in most previous studies involving altimetric data assimilation, the oceanic models were forced by a constant wind stress curl. But the main objective of this study is to explore the ability of altimeter data to complement the sampling of scatterometer winds and constrain realistically the eddy variability fields. A complementary issue which will be examined in future work is to quantify the extent to which the use of realistic wind data, as measured by scatterometer, to force ocean models is able to compensate for the inability of altimeter data to constrain properly the mean circulation in the model.

This paper is organized as follows. In the next section we summarize the properties of the oceanic model, establish the philosophy of the approach and discuss the assimilation technique used. The third section describes the simulation of data from Topex/Poseidon altimeter as well as from ERS1 and NSCAT scatterometers. The fourth section discusses the reference assimilation experiment in which the model is forced by a realistic wind stress curl derived from analyses of the ECMWF over the North Atlantic. The fifth section describes the results of the coupled experiments when altimeter data are assimilated into the model and scatterometer wind data are simultaneously used to force the model. Finally, the results are discussed in the sixth section.

MODEL AND ASSIMILATION TECHNIQUE

Simulations of the ocean circulation with simplified models based on the quasi-geostrophic formulation have shown that these models to be suitable for the reproduction of some essential features of the basin-scale variability at mid-latitudes. These models are suitable for the reproduction of some essential features of variability and under some conditions (forcing, boundary conditions) for the mean flow. Even with simplified forcing and geometry, Schmitz and Holland (1982; 1986) have pointed out that simulated eddy and mean field characteristics demonstrate striking similarities with observations in the Gulf Stream and the KuroShio. Moreover, it may be noted that this type of model is capable of reconstructing the deep flow dynamics with some realism, in particular their spectral contents, although these deep flows are only driven by pressure forces acting at the interfaces. Despite their well-known limitations, the use of such QG models to explore the impacts of altimeter data offers the advantage of (relatively) low computational costs for long runs, thereby rendering sensitivity studies possible. Furthermore, preliminary studies with primitive equation models show behavior similar to QG regarding the assimilation issue(Malanotte-

Rizzoli *et al.*, 1989). This raises the hope that the present study could be generalized, at least in part.

The multilayer QG model used here is an extension of the two-layer model by Holland (1978). The domain is a square box, 4 000 km wide, and the ocean is forced by wind stress curl. In many early mid-latitude studies the wind was constant in time, with a schematic double-cell wind pattern in space. Two main cells of large-scale circulation were created which mimic the subtropical circulation (southern gyre) and a subpolar circulation (northern gyre). A strongly inertial jet is present at mid-latitudes, associated with an intense variability field due to barotropic and baroclinic instabilities. Eddy activity is responsible for downward propagation of energy, deep eddies themselves driving a mean circulation in the subsurface ocean which could not otherwise exist (no interfacial friction is assumed between layers).

In the QG layered-model formulation, prognostic equations are written for the vorticity in each layer:

$$\partial/\partial t\,(\Delta\psi_k) = G_k \qquad (1)$$

where k is the layer number [$k \in (1, N)$]) and G_k includes all the model physics, advection, rotation, stratification, dissipation, and forcing. Dynamical topography h, appears as proportional to an explicit variable of the model, the surface stream function ψ_1, and is written as

$$h = f/g\,\psi_1 \qquad (2)$$

where f is the Coriolis parameter and g is the acceleration of gravity (subscript 1 stands for upper layer). The nudging technique of assimilation, which has already been described elsewhere (Verron and Holland, 1989 *a*) consists of modifying the upper layer equation by adding a blending term to the right-hand side:

$$\partial/\partial t\,(\Delta\psi_1) = G_1 - R\,[F(\psi_1) - F(\psi_{OBS})] \qquad (3)$$

in which F is some function of the surface streamfunction, viewed from the model (ψ_1) or viewed from the observations (ψ_{OBS}). Verron (1991) has discussed various ways of implementing the function F as the vorticity

$$\partial/\partial t\,(\Delta\psi_1) = G_1 - R\,(\Delta\psi_1 - \Delta\psi_{OBS}) \qquad (4)$$

and its form derived along satellite track (s is the local track direction),

$$\partial/\partial t\,(\Delta\psi_1) = G_1 - R\,[(\partial^2\psi_1/\partial s^2) - (\partial^2\psi_{OBS}/\partial s^2)] \qquad (5)$$

or the pure topographic height

$$\partial/\partial t\,(\Delta\psi_1) = G_1 + R\,(\psi_1 - \psi_{OBS}) \qquad (6)$$

or the residuals (or perturbations) of the previous ones

$$\partial/\partial t\,(\Delta\psi_1) = G_1 - R\,(\Delta\psi'_1 - \Delta\psi'_{OBS}) \qquad (7)$$

and

$$\partial/\partial t\,(\Delta\psi_1) = G_1 + R\,(\psi'_1 - \psi'_{OBS}) \qquad (8)$$

defining $\psi'_1 = \psi_1 - \overline{\psi}_1$ and $\psi'_{OBS} = \psi_{OBS} - \overline{\psi}_{OBS}$, where $\overline{\psi}$ represents the temporal mean streamfunction. Equations (7) and (8) require some adequate knowledge of the mean sea level, which is, as said before, a major problem when considering satellite altimetric data. In practice, one would probably have to base simulations on a reference composite mean sea level derived from the best possible model driven by the best possible (wind and thermal) forcing, associated with direct *in situ* measurements or the results of inverse methods. In any case, knowledge of the forcing is a crucial aspect which emphasizes the importance of possibly coupling altimeter and scatterometer data.

Finally, one can also consider the sea-level tendency, *i. e.* the successive time-difference in topographic height

$$\partial/\partial t\,(\Delta\psi_1) = G_1 + R\,\partial/\partial t\,(\psi_1 - \psi_{OBS}) \qquad (9)$$

which should ideally be equivalent to

$$\partial/\partial t\,(\Delta\psi_1) = G_1 + R\,\partial/\partial t\,(\psi'_1 - \psi'_{OBS}) \qquad (10)$$

and remove the problem of reliability of the mean reference due to geoid uncertainties and orbit errors. The blending term nudges the model prediction for the upper layer variable F (ψ_1) toward the observed variable F (ψ_{OBS}). Equations for other layers are unchanged. The R coefficient measures the strength of the nudging effect. The relative weight of the physical term G_1 *versus* the nudging term - R [F (ψ_1) - F (ψ_{OBS}) depends on R but also on the distance between data and model estimate. In a permanent regime, after the model has been pushed toward the data during the initialization phase, the physical term is expected to keep its dominant role and the nudging term simply keeps the model on track. In the general case, R may be a function of space and time. Then model estimates at any position may be affected by data from any surrounding points provided from possibly previous time steps.

In any present procedure for assimilating satellite altimeter data into ocean models, data are available only along ground tracks repeated at a time interval corresponding to the satellite repeat period. Whatever the mission may be, the along-track time sampling (typically 1s) may be viewed as instantaneous compared to the repeat period and a typical model time step, as well as compared with relevant time scales for the general ocean circulation. Therefore, there will be no real need to take into account the exact instant at which data will appear along a given track. Along a single track, data will be assumed to be provided at the same instant. This is, of course, untrue for different tracks. For such along-track assimilation, R has been written in the form

$$R = R_0 \exp\,[-(\Delta t/\tau^2]$$

where Δt represents the time interval between the present instant and the time at which data capture really took place. Thus the effect of data at some instant will be felt at later times. This persistence effect is quantified by the time scale parameter, τ, whose value is thought to be of the order of the correlation scale of the flow. In the real ocean this is likely to be as variable over space as is the variability spectrum. In mid-latitudes the most outstanding feature of the circulation is the jet stream variability with correlation scales of, typically, ten days (Watts, 1983). The fine tuning of R_0 on the tracks (it is zero outside) is mostly empirical. The larger the value of R_0, the stronger the nudging constraint *versus* physics.

Simulation of altimeter data and scatterometer wind data

True wind forcing

The wind stress that is used to force the reference experiment and to simulate scatterometer winds is derived from

analyses of the ECMWF model over the North Atlantic. The original data set gives twelve months of daily wind stress over the North Atlantic, on a grid of 1.125° latitude by 1.125° longitude, from 1 August 1985 to 31 July 1986. Due to the necessary adaptation of the wind forcing to the simple geometry of the model, we do not attempt to obtain a wind field which is an exact representation of the wind over the North Atlantic. Our aim is to derive a mean forcing which resembles a two-cell wind stress curl, in order to drive a double-gyre mean flow and which has realistic variability scales.

Due to model resolution, the wind field derived from those data will have variance at large scales only. But, most of the "useful" variability of the original data is thought to be retained since for basin-scale simulation of the ocean circulation, the primary forcing is the large-scale curl of the wind stress. Moreover, the dynamical response of the model to small scale forcing was found to be weak by Barnier and Le Provost (1989) when generated through a stochastic process with a realistic spectrum. The high resolution in space of the scatterometer winds will provide values of the amplitude of the curl which are much more realistic than those given by most meteorological models. But these values will be given only along the swath.

The model forcing is derived as follows. Wind stress curl is calculated daily from the wind-stress on the 1.125° grid using a second order, finite-difference, centered scheme, and is then projected on the model square-box. The curl is then interpolated to the model-grid (20 km) using bi-linear interpolation. The annual mean curl (Fig. 1 *a*) presents the classical double cell pattern characteristic of the Northwestern Atlantic wind. The Rms (Fig. 1 *b*) show that the variance increases northward, is zonally distributed in the southern basin, and is maximum in the northern basin. The time variability (not shown) is characterized by fluctuations over periods ranging from days to weeks, the amplitude of those variations being larger during the winter. A significant annual signal is therefore contained in the data. These features are the main characteristics of the wind stress curl over the western North Atlantic as described on the basis of other ECMWF data by Barnier (1986) and Mac Veigh *et al.* (1987).

Since the forcing covers only twelve consecutive months, it is assumed that it repeats itself every year, so model simulations can be run for several-year periods. The curl field described in this section will be considered as the "true" wind forcing throughout the study. It will drive the experiments that yield the reference "real world" model solutions, and is used to simulate scatterometer forcing.

ERS1 and NSCAT scatterometer wind forcing

The period of the repeating orbit is three and 35 days for ERS1, and three days for NSCAT. With a view to future missions, it is useful to focus on the appropriateness of having antennae on one side or both sides of the satellite, *i. e.* to evaluate a three-day ERS1 mission (which corresponds to the orbital period for the first six months of the actual mission) with a one-side antenna *versus* the three-day NSCAT mission with twin antennae. The objective analysis required to fill in the gaps (*see* below) is carried out daily. Thus, we believe that for the purposes of the present study, which is to consider how the patchy undersampling of the wind peculiar to spaceborne scatterometers could be corrected by the assimilation of the altimeter data, the use of a 35-day ERS1 configuration will not bring out any significant further information with regard to ERS1 and NSCAT in their three-day configuration. Therefore, when ERS1 is referred to in the following discussion, it is to be understood that we consider only its three-day configuration.

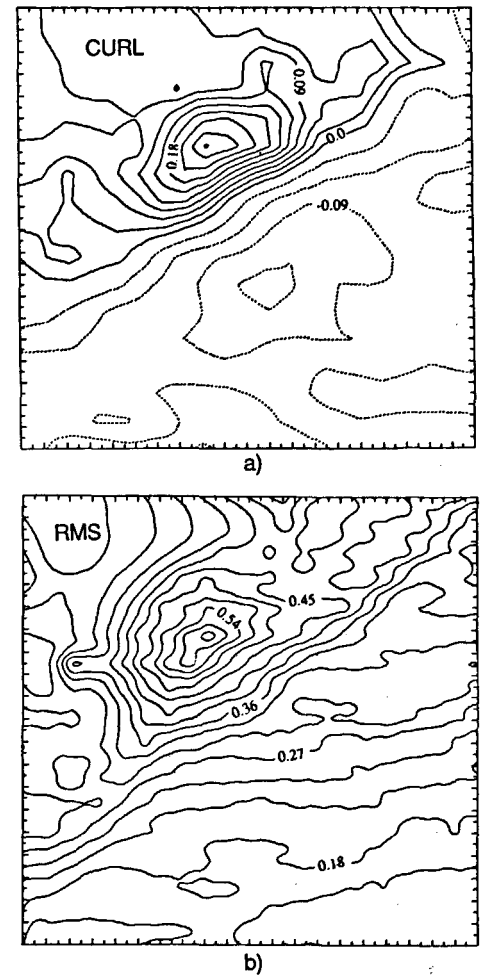

Figure 1

Wind forcing over the computational domain: a) the mean wind stress-curl; and b) the corresponding Rms. Full (dashed) contour lines indicate positive or zero (negative) values. The contour interval is CI = 3 x 10^{-2} Pa/1 000 km.

Forçage du vent correspondant au domaine de calcul : a) rotationnel moyen des tensions de vent ; et b) écart quadratique moyen correspondant. Les lignes continues (discontinues) indiquent les valeurs positives (négatives). L'intervalle entre les contours est 3 x 10^{-2} Pa/1 000 km.

Scatterometer forcings are simulated from the true wind stress curl as previously defined. The swath coverages of the ERS1 and NSCAT missions are computed over the square box domain of the model. The reader is reminded that the width of the swath is 500 km. An example of daily coverage over the 4 000 km square ocean basin is shown in

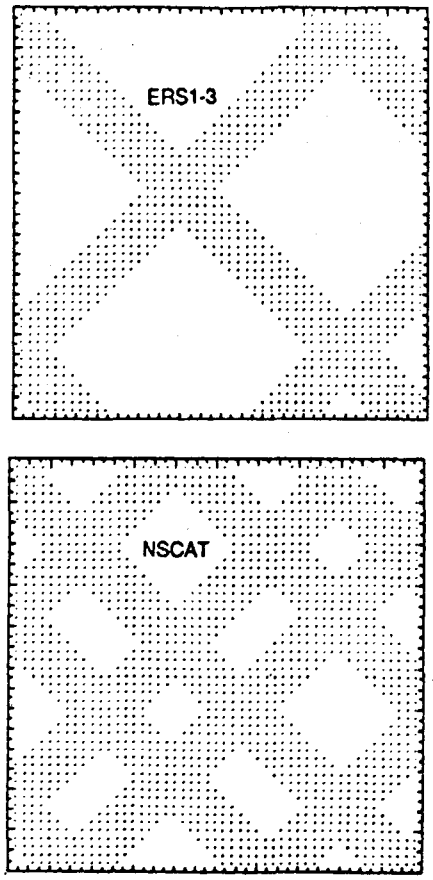

Figure 2

An example of daily coverage over the model domain by ground swaths covered by ERS1-3 and NSCAT scatterometers.

Un exemple de la couverture journalière du domaine modélisé par les fauchages des diffusiomètres ERS1 et NSCAT, dans l'hypothèse d'une période à trois jours.

Figure 2. Note that NSCAT daily coverage is close to 70 % of the modeled area, while ERS1, with only about 35 % coverage, leaves large empty regions. As for altimeter data, the simplification of the simulated ground tracking assumes rectilinear tracks over the domain, with constant crossing angle (45°) between ascending and descending orbits, *i. e.* a schematization which is close to reality in the Gulf Stream region. This leads to a spacing between two consecutive ground tracks of 740 km, close to the value for the real satellite missions at the latitude of the Gulf Stream (the actual value is 739.38 km).

The raw scatterometer wind stress curl forcing is derived as follows: for every day of the annual cycle, a daily map of the wind stress curl is constructed. The value of the forcing is that of the true curl, at grid-points located under the swath of the satellite, and is unknown at grid-points located outside the swath. The part of the domain having data every day is thus roughly twice as large in NSCAT as in ERS1, but, over a three-day period, ERS1 and NSCAT cover 87 and 94 % respectively.

In order to fill in the gaps, ERS1 and NSCAT raw wind-stress curl fields are objectively mapped. The analysis is carried out independently for every daily map of the raw forcing and uses only a small, evenly distributed number of points where the scatterometer provided data. Filling the gaps requires the correlation scale to be taken at the scale of the ground track interval (actually the correlation is chosen to be half of this interval). A Gaussian error of 5 % on the raw curl is the only statistic on the wind field itself that is included in the analysis. This approach has been shown to ensure that the largest atmospheric mesoscale features are preserved within the gaps (Barnier *et al.*, 1991). The global error estimates on the mapped fields vary between 8 and 11 %. The resulting wind stress curl fields are no longer patchy, and present continuous values at every model grid point. Hereafter, they will be referred to as the "interpolated" forcings.

Figure 3 shows the annual mean of ERS1 and NSCAT interpolated wind-stress curl. Comparison with Figure 1 *a* shows small differences between NSCAT and the true wind-stress curl patterns. These differences are not really significant compared to those observed in the different ocean-surface wind climatologies (*see* Mac Veigh *et al.*, 1987). The

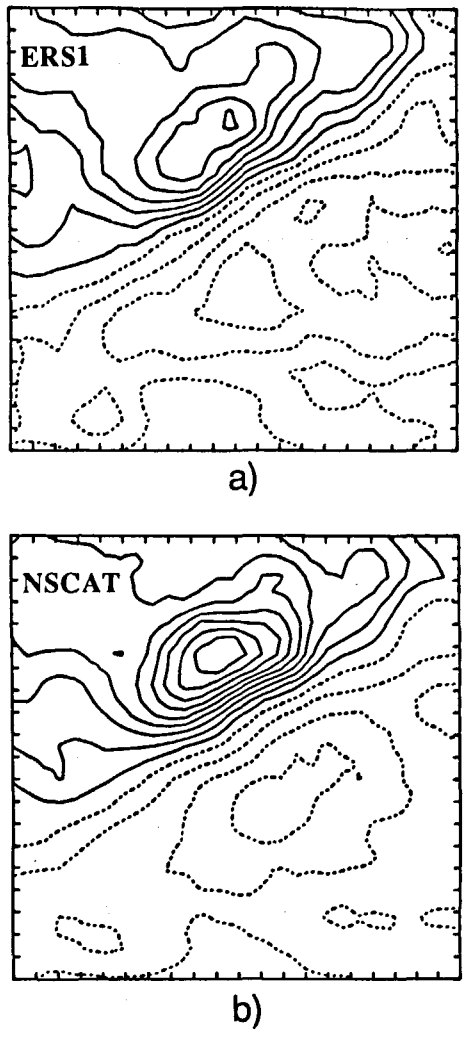

Figure 3

Annual mean of the objectively analysed wind stress-curl of: a) ERS1; and b) NSCAT. The contour interval is CI = 3 x 10^{-2} Pa/1 000 km.

Moyenne annuelle du rotationnel des tensions de vent objectivement analysées pour : a) ERS1 ; et b) NSCAT. CI = 3 x 10^{-2} Pa/1 000 km.

NSCAT wind stress curl appears smoother and the analysis increased the extension of areas of maximum curl which generally have a larger amplitude. Differences are much more prominent between ERS1 wind stress curl and the true wind stress curl; in particular, the amplitude of ERS1 wind stress curl is somewhat underestimated. These comments on the mean annual fields also hold for the daily maps (not shown here). However, the main conclusion is that, as far as the model forcing is concerned, the raw scatterometer data may be drastically improved by complementing the field in using objective analysis (Barnier *et al.*, 1991).

Altimeter data

Altimeter data are provided under the conditions of the nominal Topex/Poseidon mission, *i. e.* with a ten-day repeat orbit and the spacing between tracks is about 280 km in the east-west direction. A "historical file" of dynamical topography and flow variables in the deep layers is generated from simulation of the model forced by the "true" forcing described in "True wind forcing" section. The pseudo-Topex/Poseidon data set is provided and is also used as a reference data set (hereafter, REF) to measure the assimilation efficiency. This "real world" data set is available at every grid point in the computational domain, *i. e.*, on a regular grid of 20 km on a side.

To sample the data set to be used as along-track data, several approximations are made. Firstly, we simplify by assuming that the track intervals are constant and equal to their actual values at the latitude of the Gulf Stream mean axis, *i. e.*, 37.5° N. The ground tracking is such that the crossing angle between ascending and descending orbits is constant with latitude and equal to 45°, and that ground tracks also cross meridians (or parallels) at an angle of 45°. This approximation is close to reality in the Gulf Stream region and allows an exact fit between the ground tracks and the diagonals of the model grid. The along-track spatial sampling is then carried out every $20\sqrt{2}$ km in the assimilation which is undersampling the real situation by a factor of about 4 (real sampling of about 7 km). However, due to accuracy problems, detectable wavelengths from real measurements are probably larger. A further approximation is that data time sampling is carried out every day. Each day, data are collected relative to every track portion intersecting with the model domain during this specific day. Typically, there is an average of five tracks crossing the basin each day (Fig. 4). This approximation in time by daily sequences is necessary in order to limit the amount of data storage. We believe that it has no dramatic consequences because faster time scales than one day are not informative at oceanic standards, especially in the QG approximation which filters out high frequencies. However, the right sequencing is assumed for the ground tracks which appear in the domain exactly in the order they will appear in reality.

Assimilation in a model forced by a variable wind-stress curl

In most early mid-latitude studies involving altimetric data assimilation, the oceanic models were forced by a constant wind stress curl. The first question which arises is: how sensitive is the assimilation of the altimeter data for reproducing the ocean circulation to the use of such realistic wind stress forcing ? A first series of experiments where the along-track vorticity is assimilated (experiment True, *see* Tab. 2) was thus performed to investigate this point. It used the nudging technique described previously (*see* equation 4) and adopted the "twin experiment" procedure in order to assess the validity of the assimilation. The model parameters are presented in Table 1.

Assimilation is performed as follows: first, a simulated "real world" experiment (hereafter REF, *see* Tab. 2) is run for twenty years to provide the observations to be assimilated and to give a complete description of the four-dimensional circulation sought in subsequent assimilation experiments. Then the "assimilation experiment" is carried out in which surface data alone are made available from REF experiment. The altimeter data are extracted when a statisti-

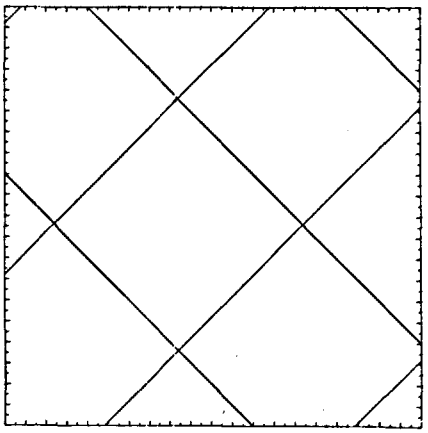

Figure 4

An example of daily coverage over the model domain by ground tracks traced out by a satellite in the nominal Topex-Poseidon mission scenario as schematized in the model.

Un exemple d'une couverture journalière du domaine modélisé par les traces au sol d'un satellite dans la configuration de la mission de Topex/Poseidon.

Table 1

Parameters of the numerical experiments.

Paramètres physiques et numériques du modèle.

Basin size		
L	km	4 000
Vertical structure		
H_1	m	300
H_2	m	700
H_3	m	4 000
g'_{12}	m/s^2	0.0162
g'_{23}	m/s^2	0.0357
Lateral friction		
A_4	m^4/s	8.10^9
Bottom friction		
ϵ	s^{-1}	10^{-7}

Table 2

References and characteristics of the different experiments.

Référence et caractéristiques des différentes expériences numériques.

Reference	Quantity to be assimilated	Wind stress forcing
REF	No assimilation	True wind stress curl
TRUE	$\Delta\psi_1 - \Delta\psi_{OBS}$	True wind stress-curl
ERS1	$\Delta\psi_1 - \Delta\psi_{OBS}$	ERS1-scatterometer interpolated
NSCAT	$\Delta\psi_1 - \Delta\psi_{OBS}$	NSCAT-scatterometer interpolated wind-stress-curl
SL	$\psi_1 - \psi_{OBS}$	NSCAT-scatterometer interpolated wind stress curl
SLTD	$\partial/\partial t\ (\psi_1 - \psi_{OBS})$	NSCAT-scatterometer interpolated wind stress curl
CB	$\alpha\ (\psi_1 - \psi_{OBS})$ + $(1 - \alpha)\ \partial/\partial t\ (\Delta\psi_1 - \Delta\psi_{OBS})$	NSCAT-scatterometer interpolated wind stress curl
SLR	$\psi'_1 - \psi'_{OBS}$	NSCAT-scatterometer interpolated wind stress curl
VR	$\Delta\psi'_1 - \Delta\psi'_{OBS}$	NSCAT-scatterometer interpolated wind stress curl

cal equilibrium is reached, *i. e.* when the downward eddy transfer of energy balances the input by the wind. The initial condition of the assimilation experiment is arbitrarily different from the simulated real world one. The efficiency of the assimilation process is measured by comparing the time evolution of the two experiments. Because the observations are taken here from the simulation by the same model as the assimilation one, the observations and model predictions are consistent (later, when using scatterometer winds this consistency will no longer be maintained). However, the observations are taken from a "historical file" at a different time from the assimilation starting point (the time lag is ten years), and the fields are completely uncorrelated when the assimilation experiment is started. The surface data height stored at every grid point in space and every day in time were then assimilated in all our experiments along only the actual tracks and weighted in time in a model with different initial conditions in which the mesoscale variabilities are completely uncorrelated (Fig. 5).

The right hand boxes of Figure 6 show the instantaneous streamfunction at the surface, intermediate and bottom layers after two years of assimilation, while the left hand boxes show the control run streamfunctions at the same time. The comparison shows that in the western basin, the circulation patterns of the former are visually similar to those of the latter, particularly in the upper layer where the location of highs and lows are faithfully reproduced. Careful inspection shows that the deep circulation patterns are rather different from the reference ocean patterns, with the relative locations of different features reproduced only approximately. In particular, there is a different shape for the recirculation south of the Gulf Stream-like jet and in the eastern basin. Intensities of flow differ by as much as 20 % in the upper layer and the discrepancy becomes more pronounced with depth where now the eddy intensities in the recirculation south of the stream differ by as much as 35 % in amplitude. However, the largest differences occur in the east where the amplitude is greatly underestimated. In these regions, the assimilation does not seem to be able adequately to drive much of the ocean variability.

This visual impression is confirmed by computing the global Rms differences in the streamfunction fields as between the assimilation experiment and the reference ocean over the entire 730 days' run (Fig. 7). The surface layer flows converge regularly towards the observations with a final Rms error of about 65 % which drops mostly during the first ten days, while the deep layers do not converge. Actually, after a slow decrease during the first 290 days, the Rms error in the deep layers suddenly increases. Afterwards, it decreases again from day 340 until day 650 from which it starts to increase. This growth of the Rms occurred approximately at the same period of each year of assimilation, and as the forcing covers only twelve consecutive months, it is presumed to repeat itself every year. Therefore, it appears that this behavior is strongly related to the annual variability of the wind stress curl. Figure 8 presents the time evolution of energy input by the wind forcing in the upper layer defined as $\langle\psi_1 \mathrm{curl}\tau\rangle$, where $\langle\ \rangle$ means basin averaged. Its behavior is particularly dominated by two peaks centered on day 265 and day 285, which could characterize a strong "weather" event and corresponds to the observed assimilation divergence at similar instants. Apparently, the assimilation of the altimeter data is inefficient in constraining the rapid response of the ocean model excited by such a forcing. The Rms error seems strongly correlated to this brutal input of energy (with a dephasing of about 25 days).

Let us now look at the behavior of the Rms corresponding to the three modes (barotropic, first and second baroclinic modes) given in the left hand boxes of Figure 7. The internal baroclinic modes converge quite well, while the convergence of the barotropic mode is not satisfactory, particularly when the "storm" acts. It is the dominant mode in the deep layers (in the flat bottom case) where this lack of convergence is quite apparent on Figure 7. The upper layer flows converge towards the observations with reasonable accuracy. This layer is dominated by the baroclinic modes which are less sensitive to the short period atmospheric forcing than the barotropic mode. It would appear that the strong daily variability in the wind stress-curl has excited a rapid barotropic oceanic signal, such as Rossby waves, which prevents total success of the assimilation method. At this stage, it is difficult to say how much of the error is due to orbital sampling and how much to the assimilation technique. However, the altimeter sampling is not appropriate for the description of the fast barotropic planetary basin modes.

Gaspar and Wunsch (1989), using a combination of a dynamical model representing linear barotropic Rossby waves with Geosat data from the Northwest Atlantic Ocean, have demonstrated that the barotropic Rossby waves could be esti-

Figure 5

Instantaneous pictures of initial state (day zero) of the control run REF (left) and the assimilation runs (right). a) upper boxes: surface layer streamfunction (CI = 2 x 10^4 $m^2 s^{-1}$); b) middle boxes: intermediate layer streamfunction (CI = 8 x 10^3 $m^2 s^{-1}$); c): lower boxes: bottom layer streamfunction (CI = 5 x 10^3 $m^2 s^{-1}$).

Images instantanées de l'état initial (jour zéro) de l'océan de contrôle REF (à gauche) et des expériences d'assimilation (à droite). a) en haut : les fonctions de courant de la couche de surface (CI = 2 x 10^4 $m^2 s^{-1}$) ; b) au milieu: les fonctions de courant de la couche intermédiaire (CI = 8 x 10^3 $m^2 s^{-1}$) ; c) en bas: fonctions de courant de la couche du fond (CI = 5 x 10^3 $m^2 s^{-1}$).

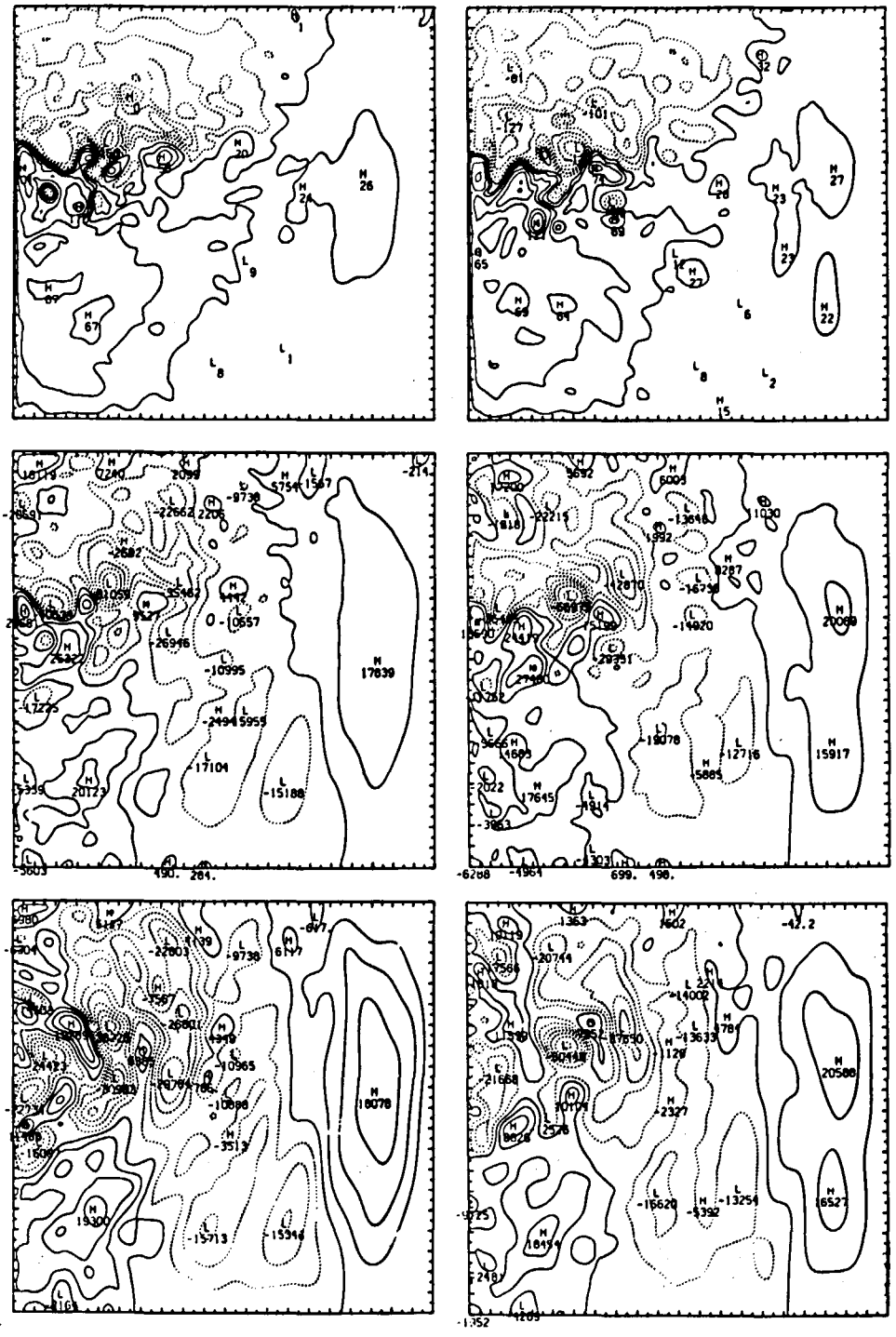

mated from altimeter data in the range of $166 < \lambda < 1\,000$ km and for periods shorter than 170 days. Here, the higher frequency wind forcing generates basin-mode Rossby waves that dominate the instantaneous barotropic streamfunction throughout the basin. The satellite sampling and/or the method of the assimilation are unable reasonably to constrain such a rapid signal. The scales under consideration here seem to fall mostly within the range of fastest basin modes (λ_x = 2 000 km, λ_y = 8 000 km, period T = 24 days and the phase velocity C_g = 80 km/day). In order to investigate this point further and to confirm our conjecture, a temporal smoothing was applied to the results described above. The left hand boxes of Figure 9 show the Rms of the three modes and the right hand boxes those of the three layers after smoothing; these Rms were computed by using a 7-day running average on ψ which appears the best time scale for the average according to the error decrease in Rms. The total percentage of Rms error is about 42 % for the surface layer, 50 % for the intermediate layer and 55 % in the bottom layer, to be compared to the corresponding numbers in Figure 7 without smoothing. The impact of filtering out the rapid barotropic signal is clear in the improvement of the convergence of the barotropic mode and the deep layers, towards the control ocean. Time sampling appears therefore as critical and there is no indication that a more sophisticated assimilation technique using same data would solve the problem.

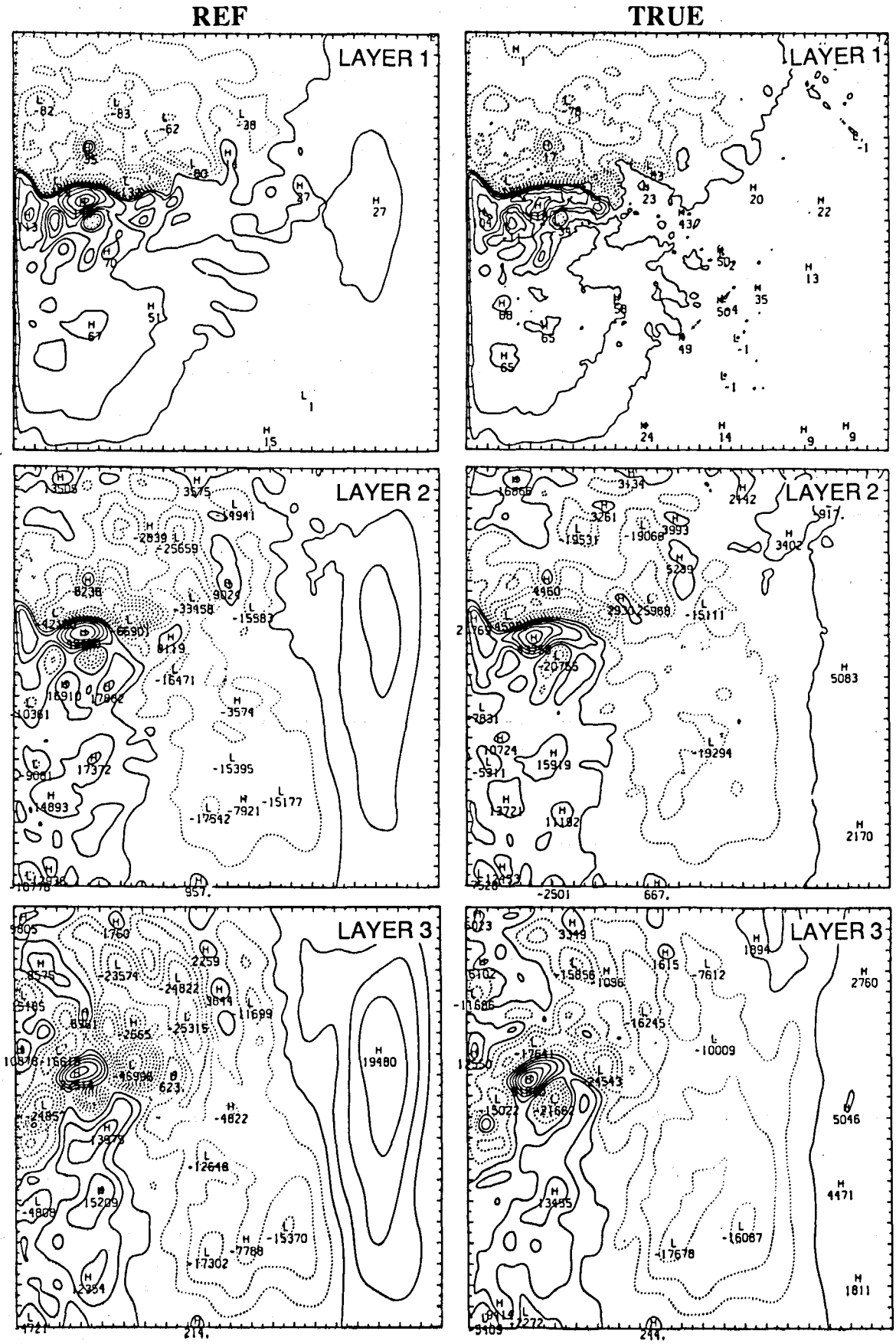

Figure 6

Instantaneous streamfunction fields after two years' assimilation in which the surface vorticity is inserted under the actual track only from data sets. From top to bottom the surface (CI = 2 x 10^4 $m^2 s^{-1}$), intermediate (CI = 8 x 10^3 m^2 s^{-1}) and bottom layers (CI = 5 x 10^3 m^2 s^{-1}) respectively are shown; a) left hand boxes: the control run (experiment REF); b) right hand boxes: the assimilation run streamfunctions (experiment TRUE).

Champs de fonctions de courant instantanées après deux ans d'assimilation pendant laquelle la vorticité de surface est insérée uniquement sous les traces. De haut en bas sont montrées respectivement les couches de surface (CI = 2 x 10^4 $m^2 s^{-1}$), intermédiaire (CI = 8 x 10^3 m^2 s^{-1}) et de fond (CI = 5 x 10^3 m^2 s^{-1}) ; a) colonne de gauche: l'océan de contrôle (expérience REF) ; b) colonne de droite : l'expérience d'assimilation TRUE. CI = 5 x 10^4 m^2 s^{-1}.

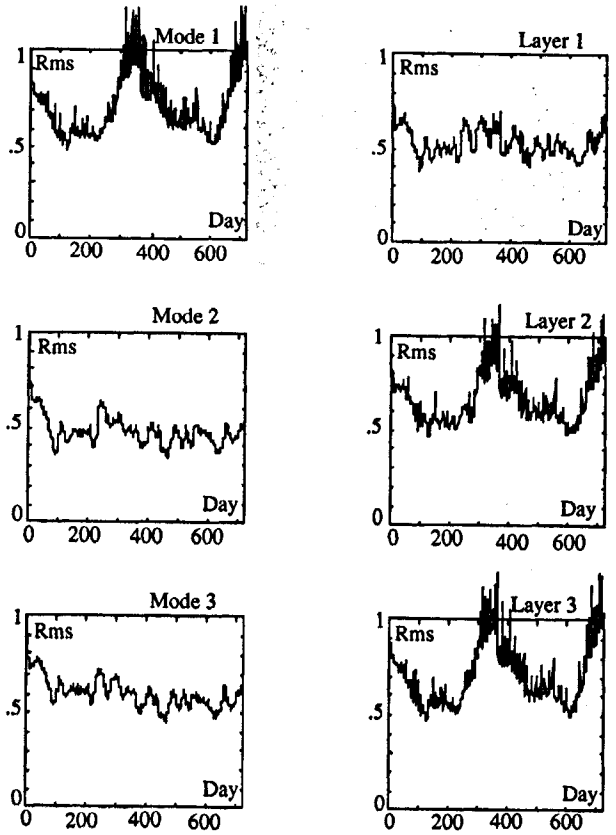

Figure 7

Time evolution of the global Rms differences between the assimilation (TRUE) and the control run (REF) streamfunctions for the three modes (left) and the three layers (right). Rms are normalized by their initial values.

Évolution en fonction du temps des Eqm entre les fonctions de courant de l'expérience d'assimilation TRUE et de l'océan de contrôle REF pour les trois modes (à gauche) et les trois couches (à droite). Les Eqm sont normalisés par leur valeur initiale.

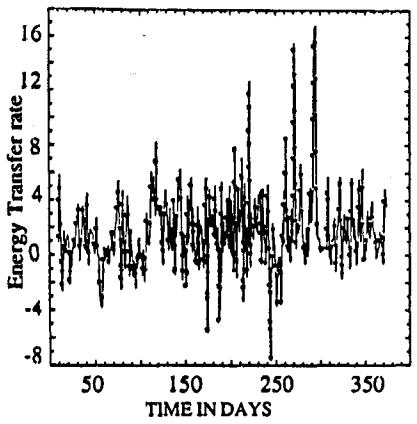

Figure 8

The time dependence of the global energy transfer rate from the wind stress curl to the upper layer of the ocean (unit is 10^{-6} m^3 s^{-3}) in experiment REF.

Évolution en fonction du temps du taux de transfert global de l'énergie du rotationnel du vent dans la couche de surface de l'océan pour l'expérience REF. L'unité est exprimée en 10^{-6} m^3 s^{-3}.

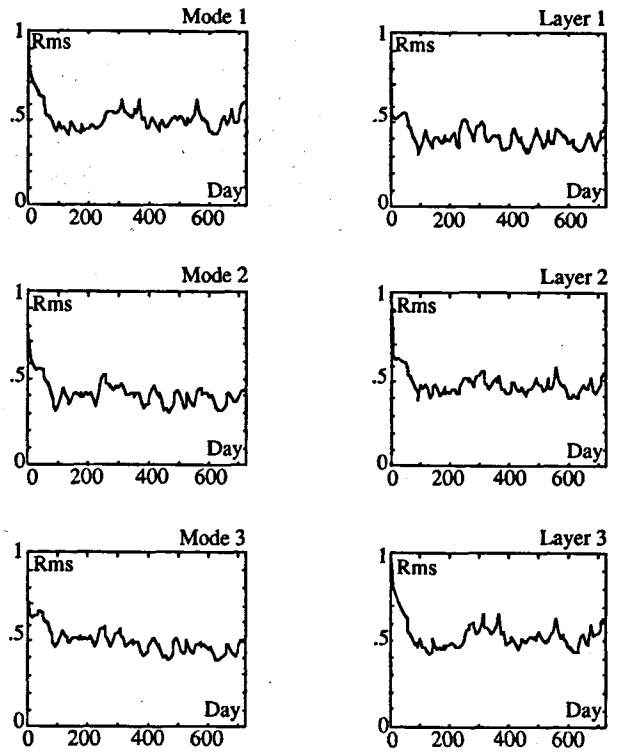

Figure 9

Time evolution of the global Rms differences between seven-day running average of the REF and TRUE streamfunctions for the three modes (left) and the three layers (right). Rms are normalized by their initial values.

Évolution en fonction du temps des Eqm entre REF et TRUE après lissage des fonctions de courant par une moyenne courante de sept jours, pour les trois modes (à gauche) et les trois couches (à droite). Les Eqm sont normalisés par leur valeur initiale.

Assimilation in a model forced by scatterometer wind data

In the second set of experiments, it is assumed that wind forcing data is provided by the scatterometer. The circulation driven by such a forcing is no longer perfectly consistent with the data. A new series of assimilation experiments (*see* Tab. 2) is performed where the model is forced either by the simulated wind stress-curl corresponding to the three-day ERS1 mission (experiment ERS1) or by the three-day NSCAT mission (experiment NSCAT). Both are compared to the control ocean REF and to the TRUE experiment where the model is forced by TRUE wind stress curl.

Assimilation of along-track vorticity data

The left hand boxes of Figure 10 show the ERS1 instantaneous streamfunctions in the three layers of the model after one year of assimilation; the middle boxes show the control ocean for comparison and the right hand boxes show NSCAT streamfunctions at the same time. The circulation patterns in the three layers for these two experiments are visually similar to those of the control ocean in the western basin, but some clear discrepancies are noticed in the east in the deep layer. Again, the most serious

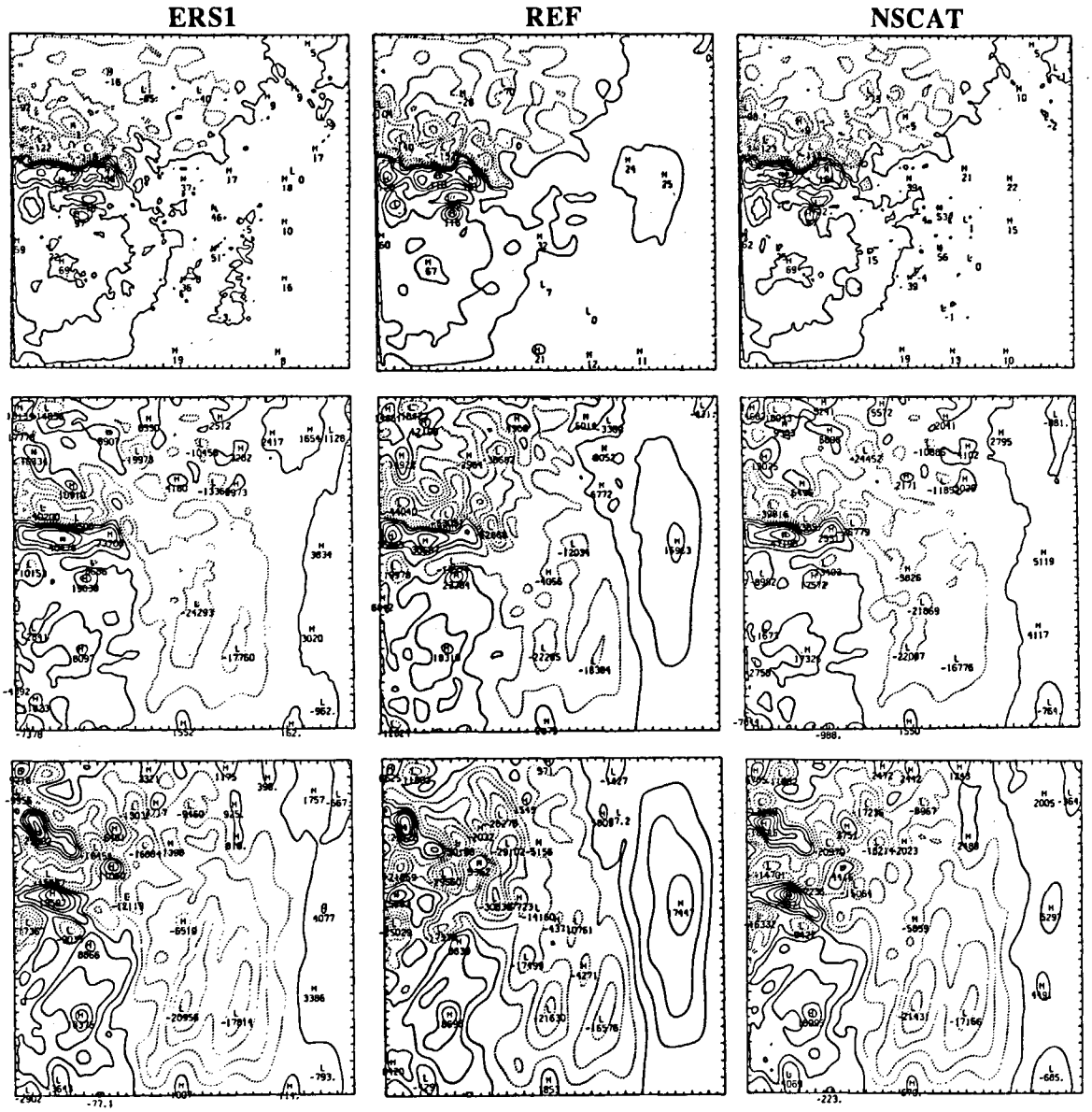

Figure 10

Instantaneous streamfunction fields after one year's assimilation in which the surface vorticity is inserted under the actual track only from data sets. From top to bottom the surface (CI = 2 x 10^4 $m^2 s^{-1}$), intermediate (CI = 8 x 10^3 m^2 s^{-1}) and bottom layers respectively are shown; a) left hand boxes: the assimilation experiment ERS1; b) middle boxes: the control run REF; c) right hand boxes: the assimilation experiment NSCAT streamfunctions (in the bottom layer CI = 5 x 10^3 m^2 s^{-1} for REF and CI = 4 x 10^3 m^2 s^{-1} for ERS1 and NSCAT).

Champs de fonctions de courant instantanées après un an d'assimilation dans laquelle la vorticité de surface est insérée uniquement sous les traces. De haut en bas sont montrées respectivement les couches de surface (CI = 2 x 10^4 $m^2 s^{-1}$), intermédiaire (CI = 8 x 10^3 m^2 s^{-1}) et du fond ; a) colonne de gauche : l'expérience d'assimilation ERS1 ; b) colonne du milieu : l'océan de contrôle REF ; c) colonne de droite: l'expérience d'assimilation NSCAT (dans la couche de fond CI = 5 x 10^3 m^2 s^{-1} pour REF et CI = 4 x 10^3 m^2 s^{-1} pour ERS1 et NSCAT)

distorsions concern the deep circulation. If the relative location of features is maintained, their intensities differ slightly in the upper layer, while differences become more important in deep layers. In the east of the basin, where the response is mainly barotropic, the amplitude of this signal is underestimated by a factor of three and one can say that the barotropic Rossby waves excited on the east are not sufficiently constrained by the assimilation of the altimeter data along the actual tracks. In any case, from this visual impression, differences between ERS1 and NSCAT forcings appear to be small.

The left hand boxes of Figure 11 show the Rms behavior in the three layers corresponding to ERS1 while the right hand boxes show those corresponding to NSCAT; these Rms are computed using a seven-day running average on ψ as was done for TRUE. The total percentage of Rms errors after one-year's assimilation for NSCAT are 46 % for the surface layer, 50 % for the intermediate layer and 53 % for the lower layer. The corresponding percentages of global Rms errors for ERS1 are 5 % higher than those of NSCAT (*see* Tab. 3). Therefore, according to our simulations, it appears that the NSCAT fields are slightly better at forcing

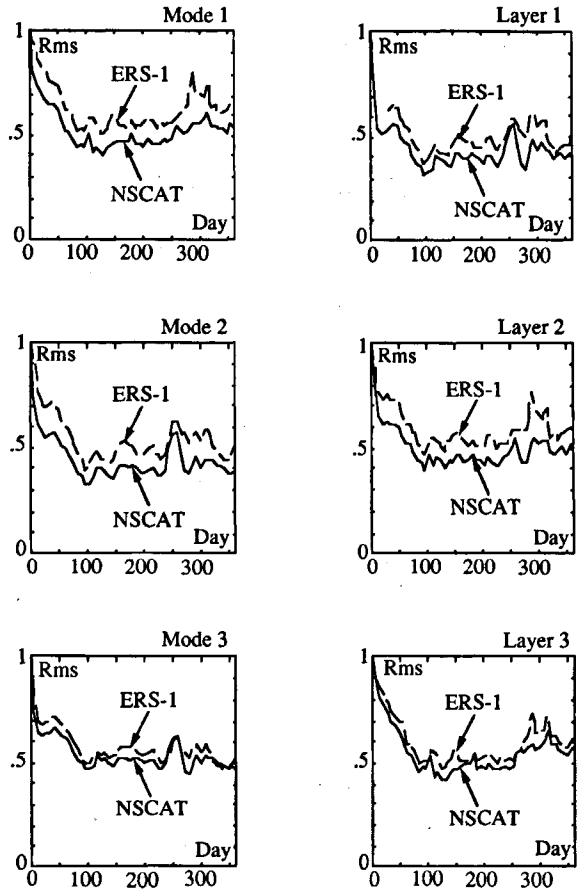

Figure 11

Time evolution of the global Rms differences between seven-day running average of the assimilation and the control run (REF) streamfunctions for the experiments ERS1 and NSCAT. Rms are normalized by their initial values.

Evolution en fonction du temps des Eqm entre les fonctions de courant (lissées par une moyenne courante de sept jours) des expériences d'assimilation et de l'océan de contrôle REF, pour les expériences ERS1 et NSCAT. Les Eqm sont normalisés par leur valeur initiale.

our oceanic model than the ERS1 ones. This is clearly due to the denser spatial coverage of the NSCAT scatterometer.

Both the comparison of the instantaneous streamfunctions and the total Rms error as between the TRUE experiment and ERS1 and NSCAT experiments indicate that the variable atmospheric forcing provided by ERS1 and NSCAT scatterometers has only a marginal impact on the ability of the model vertically to transfer the information coming from sea-surface height, although the assimilation of the altimeter data is done into a degraded ocean model. We have seen difficulties arising in the east of the basin, because of the fast barotropic Rossby waves excited by the variable wind. However, there is little difference in this regard between the true wind stress forcing and the wind stress curl provided by scatterometers. In any case, the joint use of scatterometer and altimeter data allows the flow to be kept on the "right path", *i. e.* partly to ensure this deterministic control. On the whole, it should be kept in mind, as was pointed out by Marshall (1985), that the use of simulated data overstates any realistic expectations from dynamic knowledge and gives over-optimistic results.

Table 3

Total percentage error of global Rms differences in the streamfunction fields for the various nudging experiments, after one-year assimilation. Rms were computed by using a seven-day running average on ψ.

Écart quadratique moyen total sur les fonctions de courant (lissées par une moyenne courante de sept jours), pour les différentes expériences d'assimilation, après un an d'intégration.

Reference	Surface layer	Middle layer	Bottom layer
TRUE	42	50	55
ERS1	52	54	58
NSCAT	46	50	53
SL	39	46	52
SLTD	80	75	65
SLR	58	60	60
VR	62	63	60

Assimilation of along-track sea-level data

Let us consider now the assimilation of the pure sea-level data instead of the vorticity as was the case for our previous experiments. The reference mean for this "complete" altimetric sea-level could be provided, in a real situation,

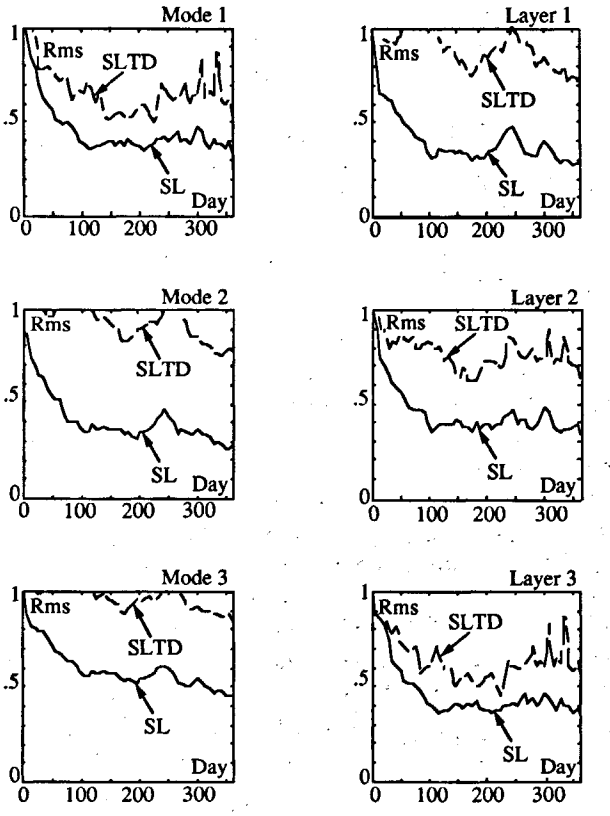

Figure 12

Time evolution of the global Rms differences between seven-day running average of the assimilation and the control run (REF) streamfunctions for the experiments SL and SLTD and where the assimilation run is forced by the interpolated NSCAT wind stress curl. Rms are normalized by their initial values.

Evolution en fonction du temps des Eqm entre les fonctions de courant (lissées par une moyenne courante de sept jours), de l'océan de contrôle REF et des expériences d'assimilation SL et SLTD qui sont forcées par le rotationnel du vent interpolé de NSCAT. Les Eqm sont normalisés par leur valeur initiale.

either from the model or from composite information including observations from various origins. In the following, we consider only the case where the model is forced by NSCAT interpolated wind stress curl. Three experiments were carried out (Tab. 2): the first with the assimilation of the complete sea level (equation 6) referred to as SL, the second with a sea-level time difference (equation 9) referred to as SLTD, and the third with a combination of sea-level and sea-level time difference referred to as CB.

Results are shown in Table 3 for the percentage of the global Rms errors between model and observation streamfunctions (computed by using a seven-day running mean on ψ) in the three layers of the model, after one year's assimilation. As before, these percentages are the average Rms over the last 100 days of the one-year assimilation experiment. Figure 12 shows the time evolution of the global Rms error in the three layers and for the three modes for the experiments described before. As pointed out by Verron (1991), the assimilation of sea-level may be as efficient as the vorticity in constraining the model towards the observations. This assessment is confirmed here for the global Rms (Tab. 3) and by analysing the instantaneous streamfunctions (not shown here). Moreover, inspection of Figures 11 and 12 reveals that nudging on sea-level is significantly more efficient than nudging on vorticity. This difference was not apparent with idealized constant wind-stress forcing (Verron, 1991). One advantage of using sea level instead of the vorticity is, that there is no need for differentiating data along the track and consequently, the satellite altimeter information is directly inserted into the model based on the QG formulation.

The use of the sea-level time difference (experiment SLTD) does not greatly improve matters except for the amplitude of the deep flow within the eastern basin. This local improvement is attributed to the fact that, unlike the other nudging equations, this form of nudging function (equation 9) introduces no dephasing. Although the altimeter data is being assimilated at the surface, the convergence of the bottom layers is more satisfactory because the control of the barotropic mode is more efficient than the convergence of the internal modes. Verron (1991) revealed that the use of the sea-level time difference could be more successful in the long term (more than two years), *i. e.* the time necessary to constrain the internal modes which have large time scales. In terms of using the realistic satellite altimeter data, such a method might be of importance in as much as it removes the geoid errors.

Combining sea-level information and sea-level time difference (experiment CB) gives the best results, although it is difficult to discriminate between the behavior of its global Rms (not shown here) and those corresponding to the use o sea level only. But careful inspection of the instantaneous streamfunctions in the three layers (Fig. 13) reveals that the

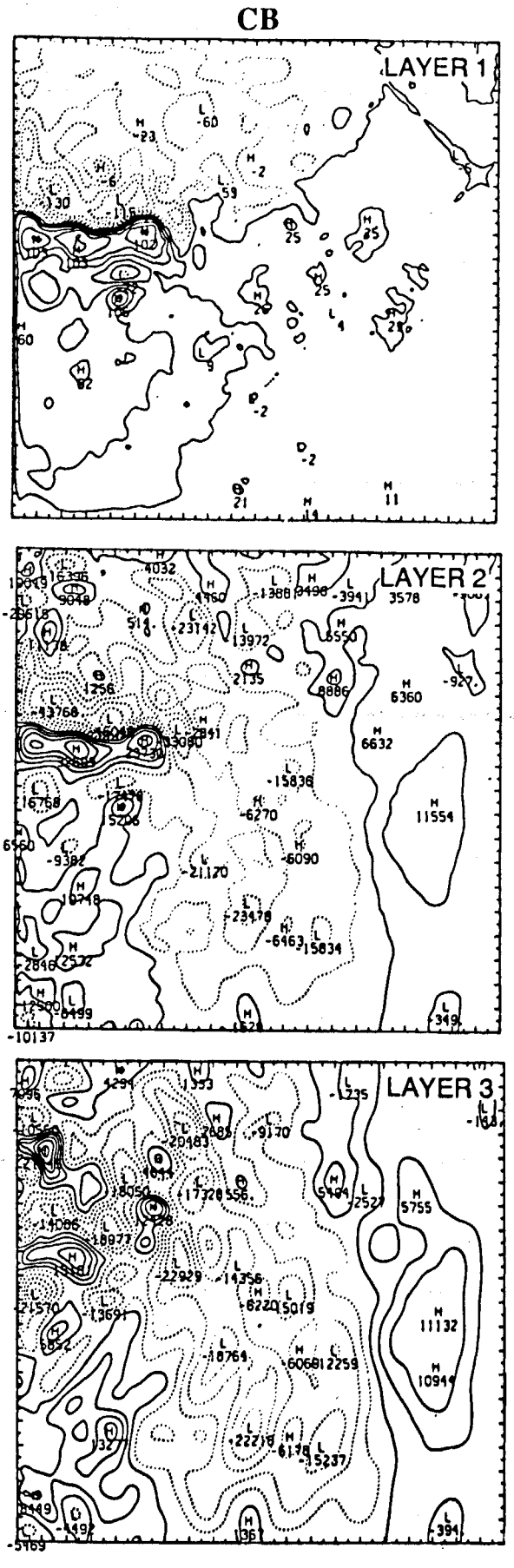

Figure 13

Instantaneous streamfunction fields after one year' assimilation in which the combination of sea level and its time difference is inserted under the actual track from datasets (CB). From top to bottom the surface, intermediate and bottom layers respectively are shown.

Champs de fonctions de courant instantanées après un an d'une expérience d'assimilation (CB) dans laquelle une combinaison du niveau de mer et de sa différence temporelle est insérée uniquement sous les traces. De haut en bas sont montrées respectivement les couches de surface, intermédiaire et de fond.

amplitude of the eastern basin is the closest to the reference. The circulation south of the jet-stream is reproduced quite nicely; in particular the location and the amplitude of the three heights located just under the jet are faithfully reproduced, which is not the case for all the previous experiments. This improvement is attributed to the fact that the two approches are complementary: the sea level ensures greater control of the amplitude and the sea-level time difference avoids some dephasing effects, in particular in the eastern basin

Assimilation of the along-track sea-level residuals

Our interest here lies in investigating the level of efficiency to be expected from using only the residuals from the complete signal, *i. e.* a signal from which the mean has been removed. In real situations, this signal constitutes the only one whose accuracy is likely to be acceptable, since the methods developed to infer or remove the mean reference are in general not accurate enough to give any reliable information on the mean sea surface topography from the data to be assimilated.

Experiments were carried out considering the assimilation of residuals instead of the complete simulated satellite altimeter data (Tab. 2). Figure 14 and Table 3 show that the assimilation of satellite altimeter residuals, either by nudging on the residuals of the sea level or of the vorticity, provides less satisfactory results. This is due to the fact that the mean sea level provided by the model as driven by NSCAT wind data, is different to some extent from the real mean sea level since, as was shown in the preceding section, the local amplitude of the NSCAT forcing is slightly different from that of the true forcing, at least outside the swaths. Consequently, and as shown by Barnier *et al.* (1991), such forcing drives a mean circulation slightly different in amplitude from that obtained with the true forcing which provides, in the present study, the real mean sea level. Table 3 shows that the small difference between the mean provided by the NSCAT and the mean provided by REF is immediately conveyed by a deterioration of the convergence of the model flow towards the observations. The Rms errors (Fig. 14) reached after a one-year assimilation are approximately 10 % higher than those obtained when the complete signal is used. In particular, it may be noted that the major discrepancy occurs in the region of the Gulf Stream detachment where the dynamic is strongly nonlinear. As discussed by Webb and Moore (1986), this limit occurs in the nonlinear portions of the model domain because the assimilation of observations into the model cannot totally preserve the instability processes and advective processes contained within the control model integration. However, in the present case careful inspection of the instantaneous streamfunctions (not presented here), shows that the assimilation of the residuals can be efficient enough to deterministically reproduce some variability features such as mesoscale, coherent eddies. From this point of view, the use of residuals can slightly correct the mean of the model, since in some regions, the mean circulation is associated to eddy variability (eddy-driven mean circulation). At this juncture, we believe that it is difficult to quantify the impact of such corrections on the improvement of the mean provided by the model. At all events, if the model yields completely wrong mean, the assimilation of the residuals is not efficient enough to reasonably constrain the mean circulation (Verron, 1991).

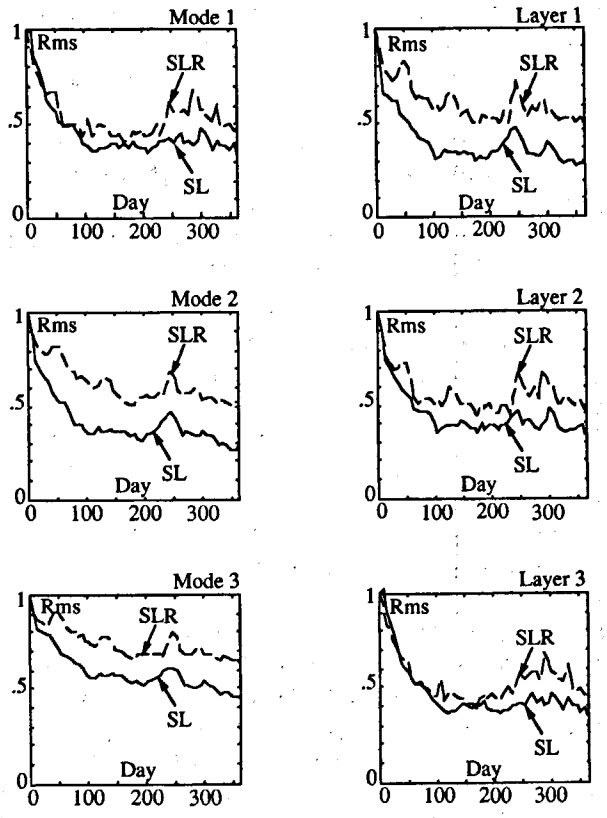

Figure 14

Time evolution of the global Rms differences between seven-day running average of the assimilation and the control run (REF) streamfunctions for the SL and SLR experiments.

Évolution en fonction du temps des Eqm entre les fonctions de courant (lissées par une moyenne courante de sept jours), de l'océan de contrôle REF et des expériences d'assimilation SL et SLR. Les Eqm sont normalisés par leur valeur initiale.

DISCUSSION

In this study we have begun to look at ways of jointly incorporating altimeter data and scatterometer wind data into an eddy resolving, multilayer ocean model based on the quasi-geostrophic formulation. Our motivation is the potential represented by both the forthcoming Topex/Poseidon altimeter dataset, which will provide synoptic maps of sea surface height variability with global coverage, and ERS1 and NSCAT scatterometer data, which will furnish mesoscale maps of ocean-surface wind intensity and direction.

In the first part, the model is forced with daily, realistic wind stress-curl in order to determine quantitatively how sensitive the efficiency of the assimilation may be to wind-stress variability. Assimilation of altimeter data powerfully constrains the baroclinic, eddy resolving ocean circulation, both at the surface and at depth. However, results show that

under optimal conditions (no data errors, perfect model), a single satellite makes only minor improvements in constraining the fast basin modes when strong variability at high frequencies of the wind stress is considered. Indeed the higher frequency forcing generates Rossby waves that dominate the instantaneous barotropic streamfunction throughout the basin and inhibit the assimilation. By filtering out motions with periods of less than one week, the computation of global Rms differences in streamfunction fields after one year's assimilation shows that the error decreases rapidly from its initial value even in the deep layers. This confirms the fact that the limited success of the assimilation of the altimeter data in spinning-up the deep layers in a satisfactory way is mostly due to satellite time sampling and dephasing due to the nudging technique.

In the second part, simulated scatterometer wind data are used to force the model and assimilation experiments then make use of both scatterometer and altimeter data. ERS1 and NSCAT raw wind stress-curl fields were objectively analyzed daily to extend the wind fields over the gaps between the scatterometer swaths. This analysis produces the "interpolated" daily forcing which is no longer patchy, and provides continuous values at every grid-point. Assimilation of the altimeter data looks like a serious candidate for at least the partial correction of the scatterometer undersampling effects; indeed inspection of the instantaneous flow patterns reveals that the position and the scale of eddy fields are reproduced quite nicely. Both the comparison of the total Rms error and the instantaneous streamfunctions indicate that the variable atmospheric forcing provided by ERS1 and NSCAT scatterometers has only a marginal impact on the ability of the model to transfer vertically the information coming from sea-surface height. However, as mentioned by Barnier *et al.* (1991), NSCAT fields seem to give more satisfactory results, and accordingly are more suitable for driving numerical ocean models than those of ERS1. This is due to their denser spatial coverage. However, overall differences between ERS1 and NSCAT results are significantly reduced by the assimilation of altimeter data.

On the other hand, the assimilation of residuals seems capable of reproducing the deterministic part of the circulation with some success, on condition that the mean provided by the model is not too far away from the real mean. Otherwise, as also shown by Verron (1991), residuals are incapable of constraining the mean circulation, which highlights the importance of having an appropriate mean. Consequently, the model prediction for the mean circulation cannot be constrained by satellite altimeter data except in a few regions where the mean circulation draws the bulk of its energy from the mesoscale eddies. An adequate knowledge of the wind forcing appears then to be crucial in order to drive a mean circulation that is as realistic as possible. According to a study by Barnier *et al.* (1991), such forcing could be provided by the forthcoming satellite missions dedicated to oceanography, such as ERS1 and NSCAT.

Although this initial exploration of the joint use of altimeter and scatterometer data does give some encouraging results, it is too soon to draw definitive conclusions. Indeed, the results obtained in the present study are dependent upon the forcing used as reference, from which the scatterometer winds were simulated. Consequently, any attempt to generalize our results must allow for the fact that ECMWF data are daily not instantaneous values and, spatially averaged over an area of 50 x 50 km, like real scatterometer data, and do not include the small-scale information that will characterize the latter.

It should also be kept in mind that these results depend on the space and time scales of motion in the region to be studied and, moreover, that they are linked to the assimilation technique used. Since the region considered in this study (North West Atlantic) is characterized by strong eddy activity, one might suspect that the results obtained here could be more satisfactory in other regions where the eddy field is less intense than in the Gulf Stream. Indeed, the present study, like those of Holland and Malanotte-Rizzoli (1989) and Verron (1990), shows that a lower sampling frequency may not resolve fast moving features such as the barotropic Rossby waves or rings rapidly escaping from the Gulf Stream jet. On the other hand, a decrease in spatial resolution may leave unresolved the smaller-scale features of the very energetic mesoscale eddy field in the vicinity of the Gulf Stream, which is known to be crucial in driving the deep circulation.

Much will be learned by using models with more realistic geometry. Indeed, the bottom topography, by coupling the barotropic mode with the baroclinic modes, can increase the impact of the assimilation of the altimeter data; moreover, this study suggests that the altimeter data place strong constraints on baroclinic motion, even under difficult conditions: assimilation along the actual tracks only, simple technique of assimilation, atmospheric forcing including strong daily variability, *etc.*

Acknowledgements

The authors are supported by the Centre National de la Recherche Scientifique and the Centre National d'Études Spatiales. This research was funded by contract 89/CNES/1318 and contract 90/DRET/1194. The calculations were made possible by the numerical facilities of the Centre de Calcul Vectoriel pour la Recherche in Palaiseau (France). Support for travel was provided by NATO.

REFERENCES

Barnier B. (1986). Investigation of the seasonal variability of the wind stress curl over the North Atlantic Ocean by means of E.O.F. analysis. *J. geophys. Res.*, **91**, 863-868.

Barnier B. and C. Le Provost (1989). *General circulation of the mid-latitude ocean: coupled effects of variable wind stress forcing and topography roughness on the mean circulation, Mesoscale/Synoptic structures in Geophysical Turbulence*, J.C.J. Nihoul and B.M. Jamart, editors. Elsevier, Amsterdam, 387-405.

Barnier B., M. Boukthir and J. Verron (1991). Using satellite scatterometer wind data to force a general circulation model. *J. geophys. Res.*, **96**, C12, 25-42.

Gaspar P. and C. Wunsch (1989). Estimates from Altimeter data of barotropic Rossby waves in the Northwestern Atlantic Ocean. *J. phys. Oceanogr.*, **19**, 1821-1844.

Holland W.R. (1978). The role of mesoscale eddies in the general circulation of the ocean. Numerical experiments using a wind-driven quasigeostrophic model. *J. phys. Oceanogr.*, **8**, 363-392.

Holland W.R. and P. Malanotte-Rizzoli (1989). Altimeter data assimilation into ocean model. *J. phys. Oceanogr.*, **19**, 1507-1534.

Large W.G., W.R. Holland and J.C. Evans (1991). Quasigeostrophic ocean response to real wind forcing: the effects of temporal smoothing. *J. phys. Oceanogr.*, **21**, 998-1017.

Mac Veigh J.P., B. Barnier and C. Le Provost (1987). Spectral and EOF analysis of four years of ECMWF wind stress curl over the north Atlantic Ocean. *J. geophys. Res.*, **92**, 13141-13152.

Malanotte-Rizzoli P., R.E. Young and D.B. Haidvogel (1989). Initialization and data assimilation experiments with a primitive equation model. *Dynam. Atmos. Oceans*, **13**, 349-378.

Miller R.N. (1989). Direct assimilation of altimetric differences using the Kalman filter. *Dynam. Atmos. Oceans*, **13**, 317-333.

Schmitz W.J. and W.R. Holland (1982). A preliminary comparison of selected numerical eddy-resolving general circulation experiments with observations. *J. mar. Res.*, **40**, 75-117.

Schmitz W.J. and W.R. Holland (1986). Observed and modeled mesoscale variability near the Gulf Stream and KuroShio extension. *J. geophys. Res.*, **91**, C8, 9624-9638.

Verron J. (1990). Altimeter data assimilation into ocean model: sensitivity to orbital parameters. *J. geophys. Res.*, **95**, 443-459.

Verron J. (1991). Nudging satellite altimeter data into quasigeostrophic ocean models. *J. geophys. Res.*, in press.

Verron J. and W.R. Holland (1989). Impacts de données d'altimétrie satellitaire sur les simulations numériques des circulations générales océaniques aux latitudes moyennes. *Annls Geophys.*, **7**, 1, 31-46.

Verron J., J.-M. Molines and E. Blayo (1992). Assimilation of Geosat data into a quasigeostrophic model of the North Atlantic between 20° and 50°N: preliminary results. *Oceanologica Acta*, **15**, 5, 575-583 (this issue).

Watts D.R. (1983). Gulf-Stream variability. in: *Eddies in Marine Sciences*, A.R. Robinson, editor. Springer-Verlag, New-York, 114-143.

Webb D.J., and A. Moore (1986). Assimilation of altimeter data into ocean models, *J. phys. Oceanogr.*, **16**, 1901-1913.

White W.B., C.K. Tai and W.R. Holland (1990). Continuous assimilation of simulated Geosat altimetric sea level into an eddy-resolving numerical ocean model: 1. *J. geophys. Res.*, **95**, 3219-3234.